

Theory of electric field induced one-magnon resonance in cycloidal spin magnets

S. Miyahara¹ and N. Furukawa^{1,2}

¹ *Multiferroics Project (MF), ERATO, Japan Science and Technology Agency (JST),
c/o Department of Applied Physics, The University of Tokyo, 7-3-1 Hongo, Tokyo 113-8656, Japan*

² *Department of Physics and Mathematics, Aoyama Gakuin University,
5-10-1 Fuchinobe, Sagami-cho, Kanagawa 229-8558, Japan*

(Dated: November 6, 2018)

We propose a new mechanism to induce a novel one-magnon excitation by the electric component of light in cycloidal spin states, *i.e.* so called electromagnon process. We calculated optical spectra in the cycloidal spin structures as observed in multiferroic perovskite manganites $RMnO_3$ where novel magnetic excitations induced by oscillating electric fields are observed. When symmetric spin-dependent electric polarizations are introduced, we have light absorptions at terahertz frequencies with one- and two-magnon excitations driven by the electric component of light. Our results show that some parts of optical spectra observed experimentally at terahertz frequencies are one-magnon excitation absorptions.

PACS numbers: 75.80.+q, 75.40.Gb, 75.30.Ds, 76.50.+g

Multiferroics, where ferromagnetism and ferroelectricity coexist, have attracted both experimental and theoretical interests [1, 2, 3]. Recently, ferroelectric perovskite manganites $RMnO_3$ ($R = Tb, Dy, Gd,$ and others) are especially paid attention to due to colossal magnetoelectric effects [4], since ferroelectricities are strongly associated with their cycloidal spin orders, and as a result, they have strong magnetoelectric couplings. Theoretically, such a strong coupling between the ferroelectricity and the cycloidal spin state can be understood by considering a spin-current induced polarization described by $\vec{P}_A \propto \vec{e}_{ij} \times (\vec{S}_i \times \vec{S}_j)$ [5, 6, 7]. Once the cycloidal spin state is realized, an electric polarization breaks out whose direction is perpendicular to the propagation and the helicity vectors of the cycloidal spin structure. One of the experimental evidences to confirm the spin-current scenario is that, in $RMnO_3$, the direction of polarizations can be controlled by changing the direction of the cycloidal plane with external magnetic fields [4]. For example, in $TbMnO_3$ the polarization flops from $P||c$ to $P||a$ by a magnetic field induced spin flop from bc to ab cycloidal states.

One of the hot topics in these multiferroics materials $RMnO_3$ is electric field induced spin excitations, or *electromagnon*, observed in an optical spectroscopy at terahertz frequencies [8, 9, 10, 11, 12, 13, 14]. In the pioneering work by Pimenov *et al.*, they observe magnetic absorptions in $TbMnO_3$ and $GdMnO_3$ for $E||a$ [8]. Especially, absorption around 2 meV in $TbMnO_3$ is expected to be strongly related to ferroelectricity induced in the spin-current model. In fact, the spin-current model predicts that the electric component of light perpendicular to the cycloidal spin plane, *i.e.* $E||a$ in $TbMnO_3$, can excite a one-magnon excitation [15]. Thus, excitations observed in $TbMnO_3$ were considered as such one-magnon excitations.

However, further detailed investigations revealed that

terahertz absorptions in $RMnO_3$ could not simply be understood by the theories proposed so far. Main unclear feature is concern with a selection rule in the spiral ordered phase, which does not depend on R site ions, temperature, external magnetic fields, and hence directions of spins. This is in contradiction with the prediction of the spin-current model $E \perp P$. For example, at the lowest temperature region of the spiral spin state in zero magnetic field, $P||c$ in $TbMnO_3$, and $DyMnO_3$ whereas $P||a$ in $Eu_{1-x}Y_xMnO_3$ and $Gd_{0.7}Tb_{0.3}MnO_3$ are observed, and then $E||a$ and $E||c$ absorptions are expected, respectively. However, in reality, the strongest absorptions are always observed for $E||a$ [8, 9, 10, 11, 12, 13, 14]. Moreover, recent experiments in $DyMnO_3$ confirm that, even when the polarization flops from $P||c$ to $P||a$ by the external magnetic fields, the selection rule hardly changes [12].

In this paper, we propose a mechanism of absorption originated from low-energy spin excitations induced by electric fields at terahertz frequencies based on a theory proposed for far infrared absorptions in antiferromagnets [16, 17, 18], *i.e.*, magnon absorptions due to virtual electron hoppings are taken into account while we neglect the phonon assisted magnon absorption. We assume that antiferroelectric spin-dependent polarization proportional to symmetric spin term $S_i \cdot S_j$ is dominant. As observed in Néel ordered state, the conventional simultaneous two-magnon absorption is possible even in cycloidal spin state. However, our results indicate that novel *one-magnon* absorption induced by the electric component of light is dominant in most of the cycloidal spin states. Because of the crystal structure, only $E||a$ component produces the one-magnon absorption in $RMnO_3$. We can reproduce some parts of experimental observation by considering a one-magnon absorption quite well.

The spin Hamiltonian under the external electric field

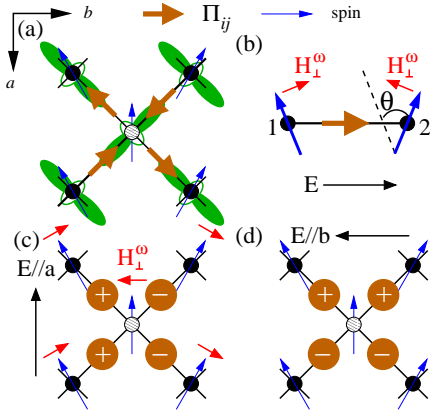


FIG. 1: (Color online) (a) Cycloidal spin structures, orbital ordering pattern on Mn site, and direction of symmetric spin dependent polarizations. (b) Non collinear spin structure on a dimer. Applying an electric field along the bond produces an effective transverse staggered fields H_{\perp}^{ω} . (c) For $E||a$, signs of $(\vec{E}^{\omega} \cdot \vec{\Pi})$ are shown on each bond. Spins are oscillated by an effective transverse fields shown by (red) arrows, which induces one-magnon resonance due to electric fields. (d) For $E||b$, signs of $(\vec{E}^{\omega} \cdot \vec{\Pi})$ are shown. The effective fields cancel out.

can be written as $H = H_0 - \vec{E} \cdot \vec{P}$, where H_0 is a spin Hamiltonian like a Heisenberg Hamiltonian, and \vec{P} is an electric dipole moment which depends on the spin configurations. In $RMnO_3$, the electric dipole moment \vec{P}_{ij} associated with a pair of spins on the nearest-neighbor bonds have been calculated by a microscopic theory for the Mn-O-Mn 180° bond [19]. In spin dependent polarizations, the symmetric spin dependent term

$$\vec{P}_S = \sum_{n.n.} \vec{\Pi}_{ij} (\vec{S}_i \cdot \vec{S}_j) \quad (1)$$

is likely dominant [18, 19]. Since such a kind of polarization is realized due to the $3x^2 - r^2/3y^2 - r^2$ orbital ordering at Mn sites, the directions of $\vec{\Pi}$ are determined as shown in Fig. 1 (a). For the cycloidal spin structure, the local symmetric spin polarization terms \vec{P}_S are aligned antiferroelectrically (see Fig. 1 (a)). This additional term does not violate the fact that the total ferroelectricity occurs solely due to the antisymmetric spin dependent term $P_A \propto \vec{S}_i \times \vec{S}_j$.

We can easily see that one-magnon can be induced by the electric component of light for noncollinear spin structures. Let us concentrate on one bond connecting site 1 and 2 (Fig. 1 (b)). When we apply the oscillating electric field \vec{E}^{ω} along the bond, Hamiltonian of the field is $-\vec{E}^{\omega} \cdot \vec{P}_s = -(\vec{E}^{\omega} \cdot \vec{\Pi}) \vec{S}_1 \cdot \vec{S}_2$. Since \vec{S}_1 and \vec{S}_2 are non-collinear, the spin \vec{S}_1 is oscillated by an effective field perpendicular to \vec{S}_1 , $H_{1\perp}^{\omega} = (E^{\omega} \cdot \Pi) S \sin \theta$. The same calculation for the spin \vec{S}_2 indicates that the effective oscillating transverse fields are staggered: $H_{1\perp}^{\omega} = -H_{2\perp}^{\omega}$. Thus,

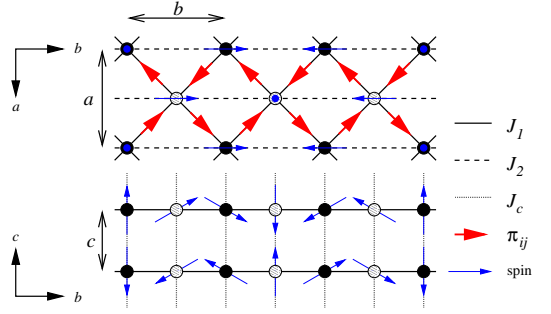


FIG. 2: (Color online) The Heisenberg model for $RMnO_3$ with nearest neighbor interactions J_1 , antiferromagnetic interactions for 2nd neighboring b direction $J_2(> 0)$, and antiferromagnetic inter layer interactions $J_c(> 0)$. The direction of $\vec{\Pi}_{ij}$ are shown by thick (red) arrows. The thin (blue) arrows describe the ground state spin configuration for the bc cycloidal state.

electric component of light can induce a one-magnon resonance caused by effective staggered transverse fields, once a noncollinear ground state is realized.

The symmetric spin dependent polarization gives us the selection rule $E||a$ straight forwardly. In $RMnO_3$, the propagation vector of cycloidal state is aligned to b directions, *i.e.*, spins along a direction are uniform. When we apply the electric field $E||a$, $\vec{E}^{\omega} \cdot \vec{\Pi}$ is uniform (staggered) along a (b) direction. As a result, electric fields couple with the spin structures. Thus, spins are oscillated with the effective staggered fields (Fig. 1 (c)), which induces one-magnon resonance. On the other hands, for $E||b$, $\vec{E}^{\omega} \cdot \vec{\Pi}$ is staggered (uniform) along a (b) direction. Staggered $\vec{E}^{\omega} \cdot \vec{\Pi}$ along a direction does not couple with the uniform spins along a direction, *i.e.*, the effective fields cancels out, and, thus, no one-magnon resonance occurs.

To proceed more quantitative argument in $RMnO_3$, let us consider the frustrated 3-dimensional $S = 2$ Heisenberg Hamiltonian as shown in Fig. 2 as the simplest model to reproduce its magnetic behaviors. J_2 and J_c are fixed to be antiferromagnetic interactions. Although J_1 is a ferromagnetic interaction in $RMnO_3$, we also extended our calculation to the antiferromagnetic J_1 region. In $RMnO_3$, interaction J_2 strongly depends R ions. Thus, we treat the ratio J_2/J_1 as a parameters and fixes the other parameters to be $|J_1| = 8$ meV, and $J_c/|J_1| = 1.5$ which well reproduces the magnetic behaviors of $RMnO_3$ including phase diagrams [20, 21]. Due to the frustration, a spiral spin state is a ground state in the parameter range $J_2/|J_1| > 0.5$ for classical spins, and a spiral angle θ is defined as $\cos \theta = -J_1/2J_2$. An anisotropy term $D \sum_i (S_i^a)^2$ is added to fix the spiral plane to be bc ($D/|J_1| = 0.2$).

At low temperatures, the magnetic behaviors of cycloidal ordered magnets can be described by the linear spin wave theory [22]. After rotations of local axis

and Holstein-Primakoff approximations, the spin Hamiltonian is written by the spin wave annihilation (creation) operator α_k^\dagger (α_k) [21]. The spin-dependent polarization is also represented by spin wave annihilation and creation operators. The polarization (1) is written as one- and two-magnon processes:

$$\begin{aligned} \vec{P}_S = & iS\sqrt{SN}\sin\theta\vec{\Pi}^{(1)}(\vec{k}_{2\pi})(\alpha_{\vec{k}_{2\pi}}^\dagger - \alpha_{\vec{k}_{2\pi}}) \\ & + iS\sin^2\frac{\theta}{2}\sum_k\vec{\Pi}^{(2)}(\vec{k}) \\ & \times \left(\alpha_k^\dagger\alpha_{-k-\vec{k}_{2\pi}}^\dagger - \alpha_k\alpha_{-k-\vec{k}_{2\pi}}\right). \end{aligned} \quad (2)$$

Here $\vec{\Pi}^{(1)}$ has only a component (see Fig 1 (c) and (d)). One-magnon absorption can be induced only for the condition $E\parallel a$ but two-magnon absorption occurs for both $E\parallel a$ and b . In the one-magnon process, magnons at $\vec{k}_{2\pi} = (2\pi/a, 0, 0)$ and $(0, 2\pi/b, 0)$ are induced and each of them has the same magnon energy $\omega_{2\pi}$. Details of $\vec{\Pi}^{(2)}$ will be reported elsewhere.

The imaginary part of complex electric polarizability tensor at $T = 0$, which represents an absorption, is obtained from Kubo formula: $\text{Im}\chi_{\alpha\alpha}(\omega) = \text{Im}\chi_{\alpha\alpha}^{(1)}(\omega) + \text{Im}\chi_{\alpha\alpha}^{(2)}(\omega)$ where

$$\text{Im}\chi_{\alpha\alpha}^{(1)}(\omega) = NS^3\Pi^2(\vec{k}_{2\pi})\sin^2\theta\delta(\omega - \omega_{2\pi})\delta_{\alpha,a} \quad (3)$$

$$\begin{aligned} \text{Im}\chi_{\alpha\alpha}^{(2)}(\omega) = & S^2\sum_k\Pi^\alpha(\vec{k})\Pi^\alpha(\vec{k})\sin^4\frac{\theta}{2} \\ & \times\delta(\omega - \omega_k - \omega_{-k-2\pi}) \end{aligned} \quad (4)$$

The first term $\text{Im}\chi_{\alpha\alpha}^{(1)}(\omega)$ represents the one-magnon absorption. The position of the absorption peak exists at a band edges at $\vec{k}_{2\pi}$. As a function of $q_0 \equiv \theta/(2\pi/b)$, one-magnon peak positions are shown in Fig. 3 (a). The second term corresponds to the absorption due to simultaneous two-magnon absorption process.

To compare the effects of one- and two-magnon processes for $E\parallel a$, integrated intensities defined as

$$I^{(\beta)} = \int_0^\infty \text{Im}\chi_{aa}^{(\beta)}(\omega)d\omega \quad (\beta = 1 \text{ or } 2) \quad (5)$$

have been calculated as a function of q_0 , respectively. The results are shown in Fig. 3 (b). Obviously, one-magnon absorption is quite strong in a wide range of parameters except for near ferromagnetic phase $q_0 \sim 0$ and antiferromagnetic phase $q_0 \sim 1$. The effects of two magnon absorption are negligible except near the Néel ordered state as read off from $I^{(2)}/I^{(1)}$ in Fig. 3 (a). The behaviors of the two magnon absorption intensity are consistent with the well-known fact that it is observed in antiferromagnets but not in ferromagnets [16, 17, 18]. We conclude that for the ferromagnetic interaction J_1 ($q_0 < 0.5$) region which $R\text{MnO}_3$ belongs to, the two-magnon absorption is negligible, contrary to our first expectation

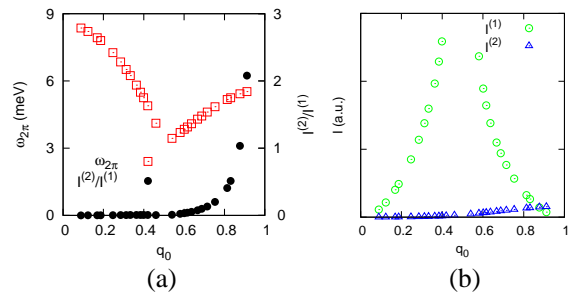


FIG. 3: (Color online) (a) The position of the delta function of a one-magnon absorption $\omega_{2\pi}$ are shown by (red) squares. $|J_1|$ is taken to be 8 meV. The ratio of $I^{(2)}/I^{(1)}$ are also plotted by filled (black) circles. (b) Intensities of one-magnon absorption $I^{(1)}$ shown by (green) circles and two-magnon absorption $I^{(2)}$ shown by (blue) triangles.

based on the magnon DOS that the absorption originates from the conventional two magnon absorption [14]. In a view point of the selection rule, dominance of this one-magnon excitation is consistent with the experimental results since light absorption occurs only for $E\parallel a$ and it is independent of the direction of the cycloidal spin plane.

Let us discuss the spectral shapes. As typical examples, we compare $\text{Im}\chi_{aa}^{(1)}$ with imaginary parts of $\epsilon\mu$ spectra in DyMnO_3 [12] and TbMnO_3 [14] on the assumption that $\text{Im}\epsilon\mu \sim \epsilon'' \equiv \text{Im}\chi_{aa}^{(1)}$. We use interactions $J_2/J_1 = -1.2$ and $J_2/J_1 = -0.8$ to reproduce cycloidal angles in DyMnO_3 ($q_0 \sim 0.36$) and TbMnO_3 ($q_0 \sim 0.29$) respectively. Calculated spectra $\text{Im}\chi_{aa}^{(1)}$ (arb. unit) together with experimental data in Refs. 12 and 14 are shown in Figs. 4 (a) and (b). Delta functions are replaced by the Lorentzian with width $\epsilon = 1$. The dispersions for magnons are shown in Fig. 4 (c). For TbMO_3 , the results are consistent with the experimental data in Ref. 23. As shown in Fig. 4 (b), our results reproduce the higher energy peak observed in TbMnO_3 at $\omega \sim 8$ meV. In addition, the shoulder structure in DyMnO_3 at $\omega \sim 5$ meV might be interpreted as one-magnon absorption as in Fig. 4 (a). However, the origin of the lower energy peaks with substantial oscillator strength around 2 meV is not clear yet. More obviously in DyMnO_3 , one-magnon absorption mechanism alone can not explain the whole spectra in $R\text{MnO}_3$.

Finally, we mention about the effects of anisotropy terms. Once the superstructure is induced by an anisotropy, one may think that such low energy peaks can be generated because a magnon at zone boundary mixes with magnons around zone center. However, satellite peaks induced by superstructures are likely too small to reproduce an experimental observation. For example, in $R\text{MnO}_3$, a spin fan structure is proposed by including the effects of anisotropy [20, 21], which explains well

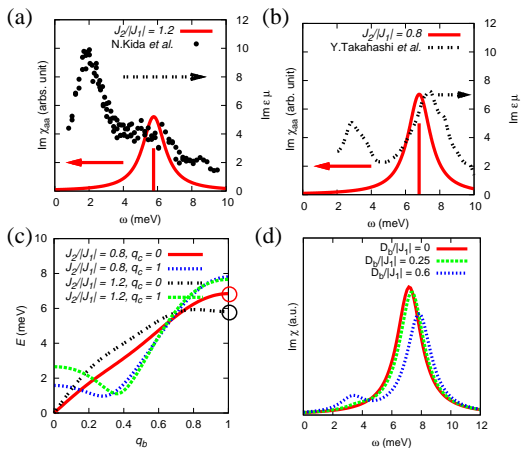


FIG. 4: (Color online) (a) Comparison of spectrum shapes for DyMnO₃ between calculation for $J_2/|J_1| = 1.2$ and experimental data $\text{Im}[\epsilon\mu]$ extracted from Ref. 12. (b) Comparison of spectrum shapes for TbMnO₃ between calculation for $J_2/|J_1| = 0.8$ and experimental data $\text{Im}[\epsilon\mu]$ extracted from Ref. 14. (c) Dispersion relation of the magnon along b direction as a function of q_b , at $q_a = 0$. Circles indicates the magnon energy induced by electric field. (c) Spectrum shapes for $J_2/|J_1| = 1/\sqrt{2}$ with an anisotropy D_b .

an elliptical modulation observed experimentally [24, 25]. Thus, we examine the effect of easy axis anisotropy along b axis $-\sum D_b(S^b)^2$ for $J_2/|J_1| = -1/\sqrt{2}$, ($q_0 = 0.25$), where a fan structure is realized. The results are shown in Fig. 4 (d). The absorption at low energies appears but the intensity is too small compared with the observed peak in TbMnO₃ even in the case for a rather strong anisotropy, *i.e.* $D_b/|J_1| = 0.6$. In this way, such an effect produces a smaller satellites and fails to explain a larger peak as in DyMnO₃ except for the unlikely case that modulations of the cycloidal spin structure are extremely large.

So far, it has been believed that the electric component of light can not induce a one-magnon resonance in Heisenberg systems through $\vec{S}_i \cdot \vec{S}_j$, because the symmetric spin polarization (1) conserves the total spin moment as seen in a two-magnon absorption in Néel ordered state [16, 17, 18]. However, we can now predict that one-magnon resonances can be induced by oscillating electric field even in some non-collinear Heisenberg system. This becomes possible because the ground state itself is symmetry broken, which makes a matrix element between ground state and one-magnon excitations non-zero. In this paper, we have clarified that one-magnon absorption is possible for a certain type of cycloidal spin states. Moreover, one-magnon resonance might also be observed in some other non-collinear spin systems, *e.g.* canted Néel ordering state as we can imagine from Fig. 1 (b). Our results indicate the possibility that electromagnons are detectable in a wide range of materials.

In terahertz absorption in RMnO₃, a few mystery are still left as open issues. The most challenging and important point is to clarify the origin of the lower energy absorption around 2meV. Also in absorption around 5 ~ 8meV, we need a rather large damping factor to reproduce experimental results, but the reason of its largeness is not obvious. Such a rather widely spreaded spectra are also observed even in conventional magnon by the inelastic neutron scattering experiments [23], thus, that might be come from the peculiar features of the magnon in the cycloidal spin state. The $E||a$ absorption is observed even in the high temperature collinear phase, *i.e.*, paraelectric phase [12, 13]. Within the linear spin wave theory, we can not treat the collinear phase properly. However, if we assume that the collinear phase is realized as a superposition of nearly degenerate ab and bc cycloidal planes as proposed in Refs. 20 and 21, the one-magnon absorption due to symmetric term might occur even in the collinear phase within our framework.

We thank H. Katsura and N. Nagaosa for useful comment, and N. Kida, M. Mochizuki, Y. Takahashi, T. Arima, R. Shimano, and Y. Tokura for fruitful discussion. This work is in part supported by Grant-In-Aids for Scientific Research from the Ministry of Education, Culture, Sports, Science and Technology (MEXT) Japan.

Note added—Recently, we became aware of similar work by R. Valdés Aguilar [26], where they report on absorption in TbMnO₃ and indicate the existence of one-magnon absorption considering the effects of orthorhombic lattice distortions.

-
- [1] Y. Tokura, Science **312**, 1481 (2006).
 - [2] W. Eeinstein, N. D. Mathur, and J. F. Scott, Nature (London) **442**, 759 (2006).
 - [3] S.-W. Cheong and M. Mostovoy, Nat. Mater. **6**, 13 (2007).
 - [4] T. Kimura, Annu. Rev. Mater. Res. **37**, 387 (2007).
 - [5] H. Katsura, N. Nagaosa, and A. V. Balatsky, Phys. Rev. Lett. **95**, 057205 (2005).
 - [6] M. Mostovoy, Phys. Rev. Lett. **96**, 067601 (2006).
 - [7] I. A. Sergienko and E. Dagotto, Phys. Rev. B **73**, 094434 (2006).
 - [8] A. Pimenov, A. A. Mukhin, V. Y. Ivanov, V. D. Travkin, A. M. Balbashov, and A. Loidl, Nat. Phys. **2**, 97 (2006).
 - [9] A. Pimenov, T. Rudolf, F. Mayr, A. Loidl, A. A. Mukhin, and A. M. Balbashov, Phys. Rev. B **74**, 100403 (2006).
 - [10] R. V. Aguilar, A. B. Sushkov, C. L. Zhang, Y. J. Choi, S.-W. Cheong, and H. Drew, Phys. Rev. B **76**, 060404 (2007).
 - [11] A. Pimenov, A. Loidl, A. A. Mukhin, V. D. Travkin, V. Y. Ivanov, and A. M. Balbashov, Phys. Rev. B **77**, 014438 (2007).
 - [12] N. Kida, Y. Ikebe, Y. Takahashi, J. P. He, Y. Kaneko, Y. Yamasaki, R. Shimano, T. Arima, N. Nagaosa, and Y. Tokura, Phys. Rev. B **78**, 104414 (2008).
 - [13] N. Kida, Y. Yamasaki, R. Shimano, T. Arima, and

- Y. Tokura, *J. Phys. Soc. Japan* **77**, 123704 (2008).
- [14] Y. Takahashi, N. Kida, Y. Yamasaki, J. Fujioka, T. Arima, R. Shimano, S. Miyahara, M. Mochizuki, N. Furukawa, and Y. Tokura, *Phys. Rev. Lett.* **101**, 187201 (2008).
- [15] H. Katsura, A. V. Balatsky, and N. Nagaosa, *Phys. Rev. Lett.* **98**, 027203 (2007).
- [16] Y. Tanabe, T. Moriya, and S. Sugano, *Phys. Rev. Lett.* **15**, 1023 (1965).
- [17] T. Moriya, *J. Phys. Soc. Jpn.* **21**, 926 (1966).
- [18] T. Moriya, *J. Appl. Phys.* **39**, 1042 (1968).
- [19] C. Jia, S. Onoda, N. Nagaosa, and J. H. Han, *Phys. Rev. B* **76**, 144424 (2007).
- [20] M. Mochizuki and N. Furukawa (2008), e-print available at arXiv:0811.4015.
- [21] M. Mochizuki, S. Miyahara, and N. Furukawa (2008), unpublished.
- [22] B. R. Cooper, R. J. Elliott, S. J. Nettel, and H. Suhl, *Phys. Rev.* **127**, 57 (1962).
- [23] D. Senff, P. Link, K. Hradil, A. Hiess, L. P. Regnault, Y. Sidis, N. Aliouane, D. N. Argyriou, and M. Braden, *Phys. Rev. Lett.* **98**, 137206 (2007).
- [24] T. Arima, A. Tokunaga, T. Goto, H. Kimura, Y. Noda, and Y. Tokura, *Phys. Rev. Lett.* **96**, 097202 (2006).
- [25] Y. Yamasaki, H. Sagayama, T. Goto, M. Matsuura, K. Hirota, T. Arima, and Y. Tokura, *Phys. Rev. Lett.* **98**, 147204 (2007).
- [26] R. V. Aguilar, A. B. S. M. Mostovoy, C. L. Zhang, Y. J. Choi, S.-W. Cheong, and H. Drew (2008), e-print available at arXiv:0811.2966.